

# Complex counterpart of variance in quantum measurements for pre- and postselected systems

Kazuhisa Ogawa,<sup>1,\*</sup> Natsuki Abe,<sup>1</sup> Hirokazu Kobayashi,<sup>2</sup> and Akihisa Tomita<sup>1</sup>

<sup>1</sup>*Graduate School of Information Science and Technology, Hokkaido University, Sapporo 060-0814, Japan*

<sup>2</sup>*School of System Engineering, Kochi University of Technology, Tosayamada-cho, Kochi 782-8502, Japan*

(Dated: February 15, 2021)

The variance of an observable for a preselected quantum system, which is always real and non-negative, appears in the increase of the probe wave packet width in indirect measurement. We extend this framework to pre- and postselected systems, and formulate a complex-valued counterpart of the variance called “weak variance.” In our formulation, the real and imaginary parts of the weak variance appear in the changes in the probe wave packet width in vertical-horizontal and diagonal-antidiagonal directions on the quadrature phase plane, respectively. Using an optical system, we experimentally demonstrate these changes in a probe wave packet width caused by the real negative and pure imaginary weak variances. Furthermore, we describe that the weak variance can be expressed as the variance of the weak-valued probability distribution for pre- and post-selected systems. These operational and statistical interpretations support that our formulation of the weak variance is reasonable as a complex counterpart of the variance for pre- and post-selected systems.

## I. INTRODUCTION

In quantum measurements, measurement outcomes show probabilistic behavior. This characteristic is peculiar not seen in classical systems, and has been the root of many fundamental arguments in quantum theory [1]. In the quantum measurement of observable  $\hat{A}$ , the probabilistic behavior of its outcomes is characterized by the statistics such as expectation value  $\langle \hat{A} \rangle$  and variance  $\sigma^2(\hat{A})$ . These values are generally measured according to the indirect measurement model [2]. In indirect measurement, the target system to be measured is coupled with an external probe system by von Neumann interaction. Regardless of the coupling strength, the expectation value  $\langle \hat{A} \rangle$  and the variance  $\sigma^2(\hat{A})$  for the target system are obtained from the displacement of the probe wave packet and the increase of its width, respectively. In other words, the probe wave packet in the indirect measurement serves as the interface that displays the probabilistic characteristics of the target system in quantum measurement.

It is interesting that, when the target system is further postselected, the displacement of the probe wave packet shows a different value from the expectation value  $\langle \hat{A} \rangle$ . Especially, when the coupling strength is weak (weak measurement setup), the probe displacement is given by  $\langle \hat{A} \rangle_w := \langle f | \hat{A} | i \rangle / \langle f | i \rangle$  for the pre- and postselected states  $\{|i\rangle, |f\rangle\}$ , which was formulated as the weak value [3]. The weak value is complex in general and can exceed the spectral range of  $\hat{A}$ . Nevertheless, by regarding the weak value as a complex counterpart of the expectation value for the pre- and postselected system, new approaches

to fundamental problems in quantum mechanics involving pre- and postselection has been investigated, such as various quantum paradoxes [4–10], understanding of the violation of Bell inequality using negative probabilities [11], the relationship between disturbance and complementarity in quantum measurements [12–14], verification of the uncertainty relations [15–17], observation of Bohmian trajectories [18, 19], and demonstration of the violation of macrorealism [20, 21].

Similar to the relation between the weak value and the expectation value, does there exist a counterpart of the variance for pre- and postselected systems? The key to this research is the function of the probe wave packet in indirect measurement as an interface that displays the characteristics of the target system. As mentioned earlier, the variance  $\sigma^2(\hat{A})$  for a preselected system appears in the increase of the probe wave packet width in indirect measurement, and due to the non-negativity of the variance, the wave packet width never decreases. For pre- and postselected systems, on the other hand, any counterparts of the variance cannot be observed in the typical framework of the weak measurement [3], in which the probe wave packet width does not change because the second- and higher-order terms of the coupling strength are ignored. Here, we focus on the recent studies reporting that when considering the second- and higher-order terms of the coupling strength the probe wave packet width can not only increase but also decrease under appropriate pre- and postselection [22, 23]. If reinterpreting the phenomena in these reports as the consequence of a counterpart of the variance for pre- and postselected systems, it may be possible to formulate an effective variance-like quantity that can be negative.

In this study, we investigate the general changes in probe wave packet width in indirect measurements for

---

\* ogawak@ist.hokudai.ac.jp

pre- and postselected systems, and based on this property, formulate a counterpart of the variance for the pre- and postselected systems. This counterpart, which we call *weak variance*, can indeed be negative and is observed as the decrease of the probe wave packet width. Moreover, the weak variance is complex in general, and can be understood by the superordinate concept of the change in the probe wave packet width on the quadrature phase plane. To demonstrate this, we performed an optical experiment observing the changes in the beam packet width in proportion to the real and imaginary parts of the complex weak variance. In addition, to help understand the outline of the weak variance, we introduce the expression of the weak variance as the second-order moment of the weak-valued probability distribution [4–13, 24–26], which is a quasi-probability distribution for pre- and postselected systems. From this agreement between the operational and statistical interpretation, our formulation of the weak variance can be considered to be a reasonable definition as a complex counterpart of the variance for pre- and postselected systems, compared to other formulations proposed previously [27–39]. Furthermore, we also formulate a counterpart of the higher-order moment, and investigate their operational and statistical meanings and applications.

## II. WEAK VARIANCE APPEARING IN INDIRECT MEASUREMENT FOR PRE- AND POSTSELECTED SYSTEMS

We first review the indirect measurement procedure using a Gaussian probe shown in Figs. 1(a) and (d), and explain that the complex weak variance appears in the latter system. The target system to be measured and the probe system are preselected in  $|i\rangle$  and  $|\phi\rangle$ , respectively. The initial probe state  $|\phi\rangle$  can be expanded as  $|\phi\rangle = \int_{-\infty}^{\infty} dX \phi(X)|X\rangle$ , where the wavefunction  $\phi(X)$  is the Gaussian distribution  $\phi(X) = \pi^{-1/4} \exp(-X^2/2)$ , and  $X$  is a dimensionless variable [40]. The observable of dimensionless position  $\hat{X}$  can be spectrally decomposed as  $\hat{X} = \int_{-\infty}^{\infty} dX X|X\rangle\langle X|$ . The time evolution by the interaction Hamiltonian  $\hat{A} \otimes \hat{K}$  is represented by the unitary operator  $\hat{U}(\theta) = \exp(-i\theta \hat{A} \otimes \hat{K})$ , where  $\hat{A} = \sum_j a_j \hat{\Pi}_j$  is the observable to be measured of the target system,  $a_j$  is an eigenvalue of  $\hat{A}$ ,  $\hat{\Pi}_j$  is the projector onto the eigenspace of  $\hat{A}$  belonging to the eigenvalue  $a_j$ ,  $\hat{K}$  is the canonical conjugate observable of  $\hat{X}$  that satisfies  $[\hat{X}, \hat{K}] = i\hat{1}$ , and  $\theta$  is a parameter with the reciprocal dimension of  $\hat{A}$ .  $\theta \|\hat{A}\|$  ( $\|\hat{A}\|$  is the largest eigenvalue of  $\hat{A}$ ) characterizes the coupling strength: if  $\theta \|\hat{A}\| \gg 1$  ( $\ll 1$ ), the coupling is considered strong (weak).

Let us consider indirect measurement of the observ-

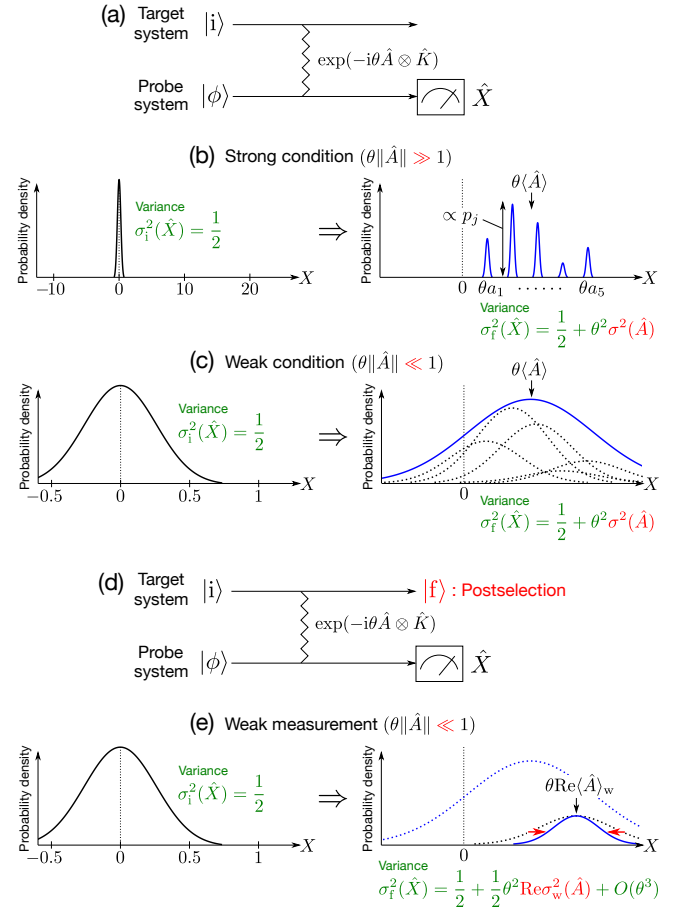


FIG. 1. (a) Quantum circuit of indirect measurement for the preselected system  $|i\rangle$ . (b) Change of the probe wave packet caused by the interaction in the quantum circuit (a) under the strong coupling condition ( $\theta \|\hat{A}\| \gg 1$ ). The distribution of the probe wave packet after the interaction reproduces the probability distribution of the outcomes in the projective measurement of  $\hat{A}$  for  $|i\rangle$ . (c) Change of the probe wave packet under the weak coupling condition ( $\theta \|\hat{A}\| \ll 1$ ), where the horizontal axis has been rescaled from (b). The variance of probe wave packet after the interaction increases in proportion to the variance  $\sigma^2(\hat{A})$ , but never decreases. (d) Quantum circuit of indirect measurement for the pre- and postselected system  $\{|i\rangle, |f\rangle\}$  (weak measurement setup). (e) Change of the probe wave packet in weak measurement circuit (d). The real part of the weak variance appears in the variance change of the probe wave packet after the postselection. Unlike the preselected system (c), the variance of the probe wave packet can decrease when the real part of the weak variance is negative.

able  $\hat{A}$  as shown in Fig. 1 (a). Suppose that we perform  $\hat{X}$  measurement in the probe system to the state after the interaction  $|\Psi\rangle := \exp(-i\theta \hat{A} \otimes \hat{K})|i\rangle|\phi\rangle$ . The probability distribution  $P(X)$  of obtaining the result  $X$  is represented as

$$P(X) = |\langle X|\Psi\rangle|^2 = \sum_j p_j |\phi(X - \theta a_j)|^2, \quad (1)$$

where  $p_j := \langle i | \hat{\Pi}_j | i \rangle$  is the projection probability of  $|i\rangle$  onto  $\hat{\Pi}_j$ . If the coupling is strong ( $\theta \|\hat{A}\| \gg 1$ ), the wave packet  $|\phi(X - \theta a_j)|^2$  for each  $j$  is well separated from each other and  $P(X)$  reproduces the probability distribution  $\{p_j\}_j$  as shown in Fig. 1(b). On the other hand, if the coupling is weak ( $\theta \|\hat{A}\| \ll 1$ ), the wave packets overlap with each other and  $P(X)$  does not reproduce  $\{p_j\}_j$  as shown in Fig. 1(c). Nevertheless, regardless of the coupling strength, the statistics of  $\hat{A}$  for the target system  $|i\rangle$ , such as the expectation value  $\langle \hat{A} \rangle$  and the variance  $\sigma^2(\hat{A})$ , can be acquired from the changes of the probe distribution  $P(X)$ . The expectation value and the variance of  $X$  for  $P(X)$ ,  $\langle \hat{X} \rangle_f$  and  $\sigma_f^2(\hat{X})$ , are respectively expressed as

$$\langle \hat{X} \rangle_f = \langle \hat{X} \rangle_i + \theta \langle \hat{A} \rangle, \quad \sigma_f^2(\hat{X}) = \sigma_i^2(\hat{X}) + \theta^2 \sigma^2(\hat{A}). \quad (2)$$

$\langle \hat{X} \rangle_i$  and  $\sigma_i^2(\hat{X})$  are the expectation value and the variance of  $\hat{X}$  for the initial probe state  $|\phi\rangle$ , respectively, and in this case,  $\langle \hat{X} \rangle_i = 0$  and  $\sigma_i^2(\hat{X}) = 1/2$ . Therefore, the expectation value  $\langle \hat{A} \rangle$  and the variance  $\sigma^2(\hat{A})$  can be measured under both strong and weak coupling conditions. We here stress that the variance of the probe wave packet after the interaction  $\sigma_f^2(\hat{X})$  never decreases due to the non-negativity of the variance  $\sigma^2(\hat{A})$ .

We next consider that the target system is pre- and postselected in  $|i\rangle$  and  $|f\rangle$ , respectively, as in Fig. 1(d). The unnormalized state of the probe system after the post-selection  $|\tilde{\phi}_f\rangle := \langle f | \Psi \rangle$  is represented as

$$|\tilde{\phi}_f\rangle = \langle f | i \rangle \left( \hat{1} - i\theta \langle \hat{A} \rangle_w \hat{K} - \frac{\theta^2}{2} \langle \hat{A}^2 \rangle_w \hat{K}^2 \right) |\phi\rangle + O(\theta^3). \quad (3)$$

The expectation value of  $\hat{X}$  for this unnormalized state  $|\tilde{\phi}_f\rangle$  is  $\langle \hat{X} \rangle_f = \langle \tilde{\phi}_f | \hat{X} | \tilde{\phi}_f \rangle / \langle \tilde{\phi}_f | \tilde{\phi}_f \rangle = \text{Re} \langle \hat{A} \rangle_w \theta + O(\theta^3)$ , where the real part of the weak value  $\langle \hat{A} \rangle_w = \langle f | \hat{A} | i \rangle / \langle f | i \rangle$  appears in the displacement of the probe wave packet, as known in the weak measurement [3]. The imaginary part of the weak value is observed in the displacement of the probe wave packet in  $\hat{K}$  basis:  $\langle \hat{K} \rangle_f = \text{Im} \langle \hat{A} \rangle_w \theta + O(\theta^3)$  [41]. By introducing the generalized position operator  $\hat{M} := \hat{X} \cos \alpha + \hat{K} \sin \alpha$  ( $\alpha \in [0, 2\pi)$ ), these relations can be summarized as

$$\langle \hat{M} \rangle_f = \left( \cos \alpha \text{Re} \langle \hat{A} \rangle_w + \sin \alpha \text{Im} \langle \hat{A} \rangle_w \right) \theta + O(\theta^3). \quad (4)$$

Now let us examine the change in the probe wave packet width. The variance of  $\hat{X}$  for  $|\tilde{\phi}_f\rangle$  is calculated

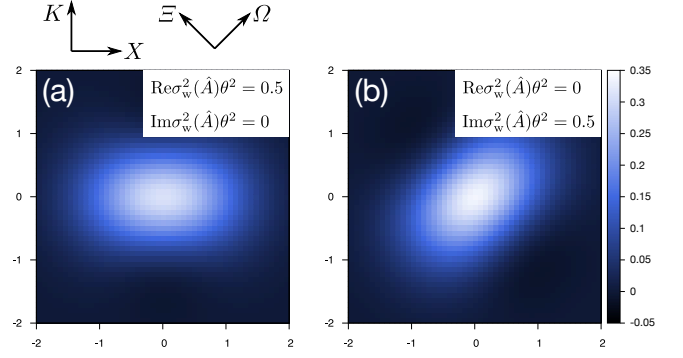


FIG. 2. Wigner functions of the normalized probe states after the post-selection,  $|\tilde{\phi}_f\rangle / \|\tilde{\phi}_f\|$ . We assume  $\langle \hat{A} \rangle_w = 0$  and neglect  $O(\theta^3)$  in Eq. (3). The horizontal and vertical axes correspond to the observables  $\hat{X}$  and  $\hat{K}$ , respectively, and the  $45^\circ$  and  $135^\circ$  axes, the observables  $\hat{\Omega}$  and  $\hat{\Xi}$ , respectively. (a) When  $\text{Re}\sigma_w^2(\hat{A})\theta^2 = 0.5$  and  $\text{Im}\sigma_w^2(\hat{A})\theta^2 = 0$ , the wave packet spreads along the  $X$  axis, while it narrows along the  $K$  axis. (b) When  $\text{Re}\sigma_w^2(\hat{A})\theta^2 = 0$  and  $\text{Im}\sigma_w^2(\hat{A})\theta^2 = 0.5$ , the wave packet spreads along the  $\Omega$  axis, while narrows along the  $\Xi$  axis.

as

$$\begin{aligned} \sigma_f^2(\hat{X}) &= \langle \hat{X}^2 \rangle_f - \langle \hat{X} \rangle_f^2 \\ &= \sigma_i^2(\hat{X}) + \frac{1}{2} \text{Re} \left( \langle \hat{A}^2 \rangle_w - \langle \hat{A} \rangle_w^2 \right) \theta^2 + O(\theta^3). \end{aligned} \quad (5)$$

The real part of the variance-like quantity appears in the quadratic term of  $\theta$ , which is ignored in the conventional weak measurement context. We define this quantity as *weak variance*  $\sigma_w^2(\hat{A})$  for  $\hat{A}$ :

$$\sigma_w^2(\hat{A}) := \langle \hat{A}^2 \rangle_w - \langle \hat{A} \rangle_w^2. \quad (6)$$

While the real part of the weak variance is similar to the normal variance in that it appears in the change in the probe wave packet width in  $\hat{X}$  basis as in Eq. (2), it can be negative unlike the normal variance; in that case, the wave packet width decreases as shown in Fig. 1(e). The decrease of the probe wave packet width reported in the previous studies [22, 23] can also be understood as the effect of the negative weak variance.

We next consider where the imaginary part of the weak variance appears. The variance of the generalized position operator  $\hat{M}$  for  $|\tilde{\phi}_f\rangle$  is calculated as [42]

$$\begin{aligned} \sigma_f^2(\hat{M}) &= \frac{1}{2} + \frac{1}{2} \left[ \cos(2\alpha) \text{Re}\sigma_w^2(\hat{A}) \right. \\ &\quad \left. + \sin(2\alpha) \text{Im}\sigma_w^2(\hat{A}) \right] \theta^2 + O(\theta^3). \end{aligned} \quad (7)$$

This equation indicates that the real and imaginary parts of the weak variance appear in the changes of the

probe wave packet width in different measurement bases. For example, when choosing  $\hat{M} = \hat{K}$  ( $\alpha = \pi/2$ ), the variance of  $\hat{K}$  for  $|\hat{\phi}_f\rangle$  is given as  $\sigma_f^2(\hat{K}) = \sigma_i^2(\hat{K}) - (1/2)\text{Re}\sigma_w^2(\hat{A})\theta^2 + O(\theta^3)$ ; that is,  $\text{Re}\sigma_w^2(\hat{A})$  also appears in the change of the wave packet width in  $\hat{K}$  basis. These relations can be understood on the quadrature phase plane as shown in Fig. 2(a). When  $\text{Re}\sigma_w^2(\hat{A}) > 0$ , the wave packet spreads along the  $X$  axis (horizontal axis), while it narrows along the  $K$  axis (vertical axis). This relationship satisfies Kennard-Robertson uncertainty relation [43, 44] up to the quadratic of  $\theta$ :  $\sigma_f^2(\hat{X})\sigma_f^2(\hat{K}) = 1/4 + O(\theta^3)$ .

On the other hand, when  $\alpha = \pi/4$ , the measured observable becomes  $\hat{M} = (\hat{X} + \hat{K})/\sqrt{2} =: \hat{\Omega}$ , which is the observable corresponding to the  $45^\circ$  axis in the quadrature phase plane of Fig. 2. From the relation  $\sigma_f^2(\hat{\Omega}) = \sigma_i^2(\hat{\Omega}) + (1/2)\text{Im}\sigma_w^2(\hat{A})\theta^2 + O(\theta^3)$ , the imaginary part of the weak variance  $\text{Im}\sigma_w^2(\hat{A})$  can be observed from the change of the probe wave packet width in  $\hat{\Omega}$  basis. Moreover, when  $\alpha = 3\pi/4$ , the measured observable becomes  $\hat{M} = (-\hat{X} + \hat{K})/\sqrt{2} =: \hat{\Xi}$ , which is the canonical conjugate of  $\hat{\Omega}$  satisfying  $[\hat{\Omega}, \hat{\Xi}] = i\hat{1}$  and corresponds to the  $135^\circ$  axis in the quadrature phase plane of Fig. 2. From the relation  $\sigma_f^2(\hat{\Xi}) = \sigma_i^2(\hat{\Xi}) - (1/2)\text{Im}\sigma_w^2(\hat{A})\theta^2 + O(\theta^3)$ ,  $\text{Im}\sigma_w^2(\hat{A})$  also appears in the change of the wave packet width in  $\hat{\Xi}$  basis. These relation can be understood on the quadrature phase plane as shown in Fig. 2(b). When  $\text{Im}\sigma_w^2(\hat{A}) > 0$ , the wave packet spreads along the  $\Omega$  axis ( $45^\circ$  axis), while it narrows along the  $\Xi$  axis ( $135^\circ$  axis). This relationship also satisfies Kennard-Robertson uncertainty relation up to the quadratic of  $\theta$ :  $\sigma_f^2(\hat{\Omega})\sigma_f^2(\hat{\Xi}) = 1/4 + O(\theta^3)$ .

### III. EXPERIMENTAL DEMONSTRATION OF OBSERVATION OF WEAK VARIANCES

To verify the existence of the effects of the weak variance, we experimentally demonstrated the observation of the weak variance using the optical system shown in Fig. 3. In this setup, the target and probe systems are polarization and transverse spatial modes of the laser beam (Menlo Systems C-fiber 780, central wavelength 780 nm), respectively. The polarization mode is a two-state system spanned by, e.g., horizontal and vertical polarization basis  $\{|H\rangle, |V\rangle\}$  or diagonal ( $45^\circ$ ) and anti-diagonal ( $135^\circ$ ) polarization basis  $\{|D\rangle := (|H\rangle + |V\rangle)/\sqrt{2}, |A\rangle := (|H\rangle - |V\rangle)/\sqrt{2}\}$ . The pre- and postselection  $\{|i\rangle, |f\rangle\}$  in the polarization mode was prepared using Glan-Thompson prisms (GTPs), a half-wave plate (HWP), and quarter-wave plates (QWPs). The initial transverse distribution of the beam's amplitude was prepared in a Gaussian distribution  $\phi(X) = \pi^{-1/4}\exp(-X^2/2)$ , where  $X$  is the

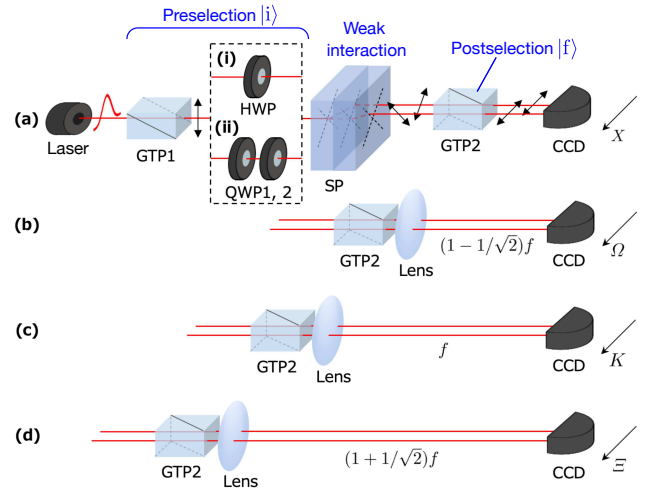


FIG. 3. Experimental setup for the observation of weak variances. GTP: Glan-Thompson prism, HWP: half-wave plate, QWP: quarter-wave plate, SP: Savart plate, CCD: charge-coupled device. (a) Experimental setup when the probe system is measured in  $\hat{X}$  basis. In the preselection, a HWP and two QWPs are used to prepare the weak variance to be (i) negative real and (ii) positive pure imaginary, respectively. (b)–(d) Experimental setups when the probe system is measured in  $\hat{\Omega}$ ,  $\hat{K}$ , and  $\hat{\Xi}$  basis, respectively. The lens (focal length  $f = 1$  m) and free space propagation perform a fractional Fourier transform on the transverse distribution of the beam.

dimensionless position variable normalized by the standard deviation of this distribution. The weak interaction  $\exp(-i\theta\hat{A} \otimes \hat{K})$  was implemented using a Savart plate (SP), which is composed of two orthogonal birefringent crystals ( $\beta$ -BaB<sub>2</sub>O<sub>4</sub>, 1 mm thickness). In our setup,  $\hat{A}$  was chosen as  $\hat{A} = |D\rangle\langle D| - |A\rangle\langle A|$  and then SP causes a transverse shift of the diagonally (anti-diagonally) polarized beam by a distance  $\theta$  ( $-\theta$ ). The probe system was finally measured in  $\hat{X}$ ,  $\hat{\Omega}$ ,  $\hat{K}$ , and  $\hat{\Xi}$  basis.  $\hat{X}$  measurement for the transverse intensity distribution of the beam was implemented using charge-coupled device (CCD) camera (Teledyne Princeton Instruments ProEM-HS:512BX3), as shown in Fig. 3(a). On the other hand, the intensity measurement in  $\hat{\Omega}$ ,  $\hat{K}$ , and  $\hat{\Xi}$  basis were implemented by fractional Fourier transforming (for detail, see Appendix B) the beam distribution using a lens (focal length  $f = 1$  m) before  $\hat{X}$  measurement by the CCD camera, as shown in Figs. 3(b)–(d).

In order to verify the effects of the real and imaginary parts of weak variance independently, we chose the pre- and postselected states  $\{|i\rangle, |f\rangle\}$  of the polarization so that the weak variance becomes (i) negative real or (ii) positive pure imaginary. In the case (i), the preselected state  $|i\rangle$  was prepared by passing the vertically polarized beam through HWP whose fast axis is rotated from the

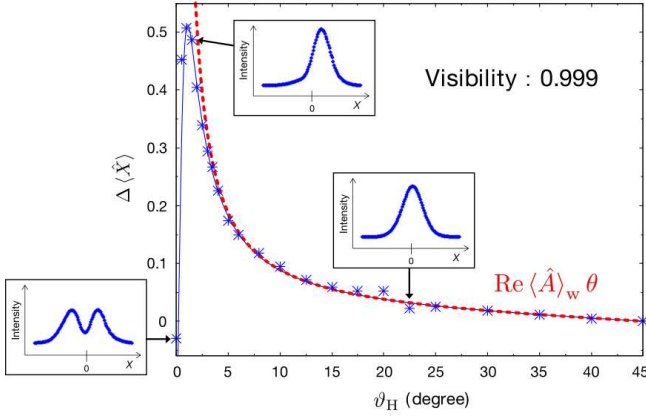


FIG. 4. Measurement results of  $\Delta\langle\hat{X}\rangle$  in the case (i). The solid blue line is the theoretical curve fitted to the measured data. The red dashed line shows the weak value  $\text{Re}\langle\hat{A}\rangle_w\theta$  ( $\theta = 0.032$ ) for various  $\vartheta_H$ . (Insets) Intensity distribution of the beam for each  $\vartheta_H$ . When  $\vartheta_H$  is close to zero, the  $O(\theta^3)$  term in Eq. (4) becomes dominant and the distribution becomes different from Gaussian.

vertical direction by the angle  $\vartheta_H$ ; the output state becomes  $|i\rangle = \cos(2\vartheta_H - \pi/4)|D\rangle + \sin(2\vartheta_H - \pi/4)|A\rangle$ . The postselected state was fixed to  $|f\rangle = |H\rangle$ . The weak value and weak variance becomes real numbers as follows:

$$\langle\hat{A}\rangle_w = \frac{\cos(2\vartheta_H)}{\sin(2\vartheta_H)}, \quad \sigma_w^2(\hat{A}) = -\frac{\cos(4\vartheta_H)}{\sin^2(2\vartheta_H)}. \quad (8)$$

In the case (ii), the preselected state  $|i\rangle$  was prepared by passing the vertically polarized beam through QWP1 whose fast axis is rotated from the vertical direction by the angle  $\vartheta_Q$  and QWP2 whose fast axis is fixed in vertical direction; the output state becomes  $|i\rangle = \cos(\vartheta_Q - \pi/4)|D\rangle + e^{-i2\vartheta_Q} \sin(\vartheta_Q - \pi/4)|A\rangle$ . The postselected state was fixed to  $|f\rangle = |H\rangle$ , as in the case (i). The weak variance becomes a pure imaginary number as follows:

$$\sigma_w^2(\hat{A}) = 2i \frac{\cos(2\vartheta_Q)}{\sin^2(2\vartheta_Q)}. \quad (9)$$

First, we observed the weak value that appears in the transverse displacement of the beam's intensity distribution. Figure 4 shows the measurement results of the displacement of the mean value of the beam's intensity distribution in the  $\hat{X}$  basis for various  $\vartheta_H$ ,  $\Delta\langle\hat{X}\rangle := \langle\hat{X}\rangle_f - \langle\hat{X}\rangle_i$ , in the case (i). When  $\vartheta_H$  is small, the pre- and postselected states are close to orthogonal and  $\Delta\langle\hat{X}\rangle$  becomes large. The blue solid line is the theoretical curve of  $\Delta\langle\hat{X}\rangle$  fitted to the measured values with the visibility  $V$  and the coupling strength  $\theta$  as fitting parameters (for detail, see Appendix C), from which  $V = 0.999$  and  $\theta = 0.032$  were decided. The red dashed line is the theo-

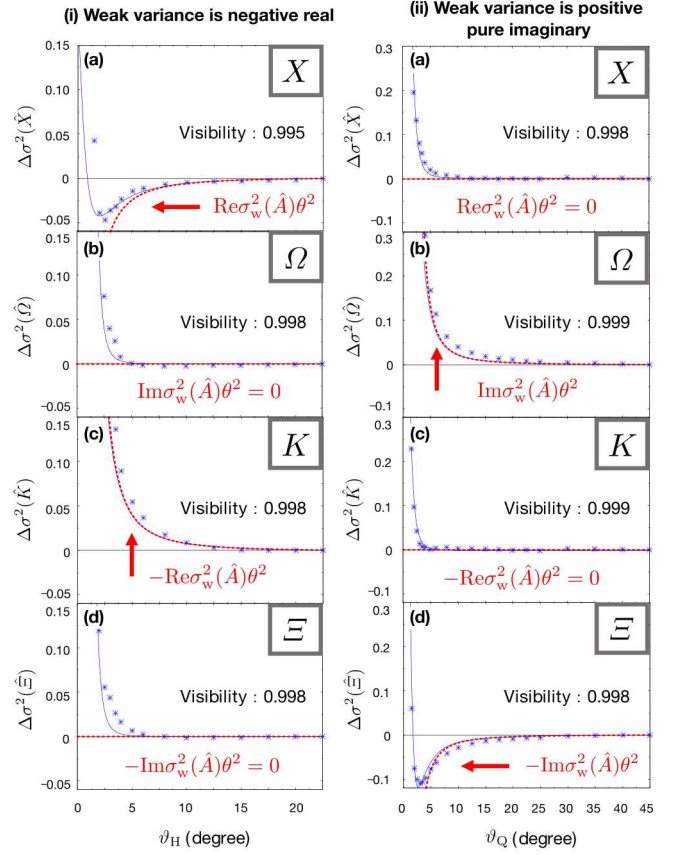


FIG. 5. Measurement results of  $\Delta\sigma^2(\hat{M})$  in the cases that (i) the weak variance is negative real, and (ii) pure imaginary. (a)–(d) Results when the measurement bases are  $\hat{X}$ ,  $\hat{\Omega}$ ,  $\hat{K}$ , and  $\hat{\Xi}$ . The solid blue lines are the theoretical curves fitted to the measured data. The red dashed lines are the theoretical curves of the weak variance  $[\cos(2\alpha)\text{Re}\sigma_w^2(\hat{A}) + \sin(2\alpha)\text{Im}\sigma_w^2(\hat{A})]\theta^2$  ( $\theta = 0.032$ ) for various  $\vartheta_Q$ .

retical curve of the weak value  $\text{Re}\langle\hat{A}\rangle_w\theta$  ( $\theta = 0.032$ ) for various  $\vartheta_H$ . Most of the measured values are consistent with this curve, which indicates that this measurements of the weak values were valid.

Next, we observed the weak variance that appears in the change of the variance of the beam's intensity distribution. Here  $\Delta\sigma^2(\hat{M}) := [\sigma_f^2(\hat{M}) - \sigma_i^2(\hat{M})]/\sigma_i^2(\hat{M})$  denotes the rate of change of the variance of the beam's intensity distribution from the initial value in the basis of  $\hat{M} = \hat{X} \cos \alpha + \hat{K} \sin \alpha$ . Figure 5 shows the measurement results of  $\Delta\sigma^2(\hat{M})$  ( $\hat{M} = \hat{X}, \hat{\Omega}, \hat{K}, \hat{\Xi}$ ) for various  $\vartheta_Q$ , in each of cases (i) and (ii). When  $\vartheta_Q$  is small, the pre- and postselected states are close to orthogonal and large variance changes were observed. The blue solid lines are the theoretical curves of  $\Delta\sigma^2(\hat{M})$  fitted to the measured values. While the fixed value  $\theta = 0.032$  was used, the visibility  $V$  was used as a fitting parameter, considering the difference in alignment in

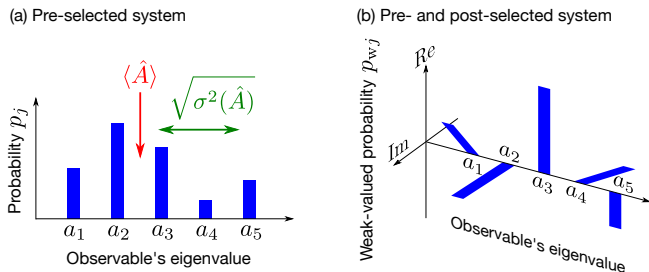


FIG. 6. (a) Probability distribution of the projective measurement of  $\hat{A}$  for a preselected system. The expectation value and variance of this distribution are  $\langle \hat{A} \rangle$  and  $\sigma^2(\hat{A})$ , respectively. (b) Weak-valued probability distribution of the observable  $\hat{A}$  for a pre- and postselected systems. The weak-valued probabilities  $p_{wj}$  are complex and expressed on the complex plane.  $\langle \hat{A} \rangle_w$  and  $\sigma_w^2(\hat{A})$  are also complex, but cannot be depicted in this graph.

each measurement (for detail, see Appendix C). The red dashed lines are the theoretical curves of the weak variance  $[\cos(2\alpha)\text{Re}\sigma_w^2(\hat{A}) + \sin(2\alpha)\text{Im}\sigma_w^2(\hat{A})]\theta^2$  ( $\theta = 0.032$ ) for various  $\vartheta_Q$  and most of the measured values are consistent with these curves. It should be noted that, in the case (i),  $\Delta\sigma^2(\hat{X})$  certainly shows negative due to the effect of the negative real weak variance; correspondingly,  $\Delta\sigma^2(\hat{K})$  increases. On the other hand, since the imaginary part of the weak variance is zero,  $\Delta\sigma^2(\hat{\Omega})$  and  $\Delta\sigma^2(\hat{\Xi})$  remain almost zero. In the case (ii), since the weak variance is positive pure imaginary,  $\Delta\sigma^2(\hat{\Omega})$  and  $\Delta\sigma^2(\hat{\Xi})$  show positive and negative, respectively. On the other hand, since the real part of the weak variance is zero,  $\Delta\sigma^2(\hat{X})$  and  $\Delta\sigma^2(\hat{K})$  remain almost zero. These results indicates that it was observed the real and imaginary parts of the weak variance appear in the change of the wave packet width according to our theory.

#### IV. STATISTICAL INTERPRETATION OF WEAK VARIANCE AS STATISTIC OF WEAK-VALUED PROBABILITY DISTRIBUTION

Here we describe that the weak variance is expressed as a statistic of the weak-valued probability distribution, which is a pseudo-probability distribution for the pre- and post-selected system. This relation is similar to that the variance is expressed as a statistic of the probability distribution for the preselected system. This statistical interpretation of the weak variance, together with the operational interpretation described above, rationalizes the definition of the weak variance as a counterpart of the variance for the pre- and postselected systems.

The weak-valued probability  $p_{wj} := \langle \hat{\Pi}_j \rangle_w$  is defined as the weak value of each element of the set of projection operators  $\{\hat{\Pi}_j\}_j$  that satisfy the completeness condition

$\sum_j \hat{\Pi}_j = \hat{1}$ . Weak-valued probabilities can be any complex number outside  $[0, 1]$ , but their sum for all  $j$  is unity:  $\sum_j p_{wj} = 1$ . By regarding the weak-valued probability as a quantity corresponding to the probability that the pre- and post-selected particle is found in the eigenspace  $\hat{\Pi}_j$  between the pre- and postselection, a probabilistic interpretation approach has been given to fundamental problems in quantum mechanics [4–10]. In addition, the negativity and non-reality of the weak-valued probabilities have played an essential role in the studies such as the investigation of the relationship between disturbance and complementarity in quantum measurement [12, 13], the explanation of the violation of Bell inequality using negative probabilities [11], quantum enhancement of the phase estimation sensitivity by postselection [24], understanding of out-of-time-order correlators as witness for quantum scrambling [25, 26].

The weak value  $\langle \hat{A} \rangle_w$  and weak variance  $\sigma_w^2(\hat{A})$  of the observable  $\hat{A} = \sum_j a_j \hat{\Pi}_j$  can be expressed as follows using the weak-valued probabilities  $\{p_{wj}\}_j$ :

$$\langle \hat{A} \rangle_w = \sum_j a_j p_{wj} \quad (10)$$

$$\sigma_w^2(\hat{A}) = \sum_j (a_j - \langle \hat{A} \rangle_w)^2 p_{wj} = \sum_j |a_j - \langle \hat{A} \rangle_w|^2 p_{wj}, \quad (11)$$

where the second equation in Eq. (11) holds when  $\hat{A}$  is Hermite. These expressions are similar to those of the expectation value  $\langle \hat{A} \rangle = \sum_j a_j p_j$  and variance  $\sigma^2(\hat{A}) = \sum_j (a_j - \langle \hat{A} \rangle)^2 p_j$  using the probability distribution  $\{p_j\}_j$ , respectively. In this sense, the weak value and the weak variance can be regarded as the expectation value and the variance for the weak-valued probability distribution, respectively. In addition, since the weak-valued probability is represented as the conditional pseudo-probability for the Kirkwood-Dirac distribution [45, 46], the weak value and weak variance are also regarded as the conditional pseudo-expectation value and the conditional pseudo-variance for the Kirkwood-Dirac distribution, respectively (for detail, see Appendix D). Furthermore, the weak value and the weak variance satisfy the equations similar to the law of total expectation and the law of total variance, respectively:

$$\langle \hat{A} \rangle = \langle i | \hat{A} | i \rangle = \sum_j |\langle f_j | i \rangle|^2 \langle \hat{A} \rangle_{wj}, \quad (12)$$

$$\sigma^2(\hat{A}) = \sum_j |\langle f_j | i \rangle|^2 \sigma_{wj}^2(\hat{A}) + \sum_j |\langle f_j | i \rangle|^2 \left( \langle \hat{A} \rangle_{wj} - \langle \hat{A} \rangle \right)^2, \quad (13)$$

where  $\langle \hat{A} \rangle_{wj} := \langle f_j | \hat{A} | i \rangle / \langle f_j | i \rangle$  and  $\sigma_{wj}^2(\hat{A}) := \langle \hat{A}^2 \rangle_{wj} -$

$$\langle \hat{A} \rangle_{wj}^2$$

So far, several definitions of the quantity corresponding to the variance for the pre- and postselected systems have been considered, such as the form of the weak variance introduced in Eq. (6) [27–31], its absolute value [32, 33], its real part [34, 39], and other forms [35–38]. Our discussion in this paper have manifested that our form of the weak variance has similarities to the normal variance in terms of both the measurement method using indirect measurement and the statistical expression using the weak-valued probability distribution. Therefore, the weak variance defined in Eq. (6) can be regarded reasonable as a counterpart of the variance for the pre- and post-selection system.

## V. CONCLUSION

In this paper, we have introduced the weak variance  $\sigma_w^2(\hat{A})$  as a complex counterpart of the variance for pre- and postselected systems. We have theoretically described that the weak variance appears in the change of the probe wave packet width in indirect measurement for pre- and postselected systems, and experimentally demonstrated it using an optical setup. We have also describe that the weak value  $\langle \hat{A} \rangle_w$  and the weak variance  $\sigma_w^2(\hat{A})$  are expressed as the statistics of the weak-valued probability distribution  $\{p_{wj}\}_j$ . These operational and statistical interpretations are similar to the expectation value  $\langle \hat{A} \rangle$  and the variance  $\sigma^2(\hat{A})$  for preselected systems. Therefore, our formulation of the weak variance can be considered to be a reasonable definition as a counterpart of the variance for the pre- and postselected systems.

The rest of this paper further extends the concept of the weak variance. We define *n-th order weak moment* of the observable  $\hat{A}$  as  $\langle \hat{A}^n \rangle_w$ . The set of the weak moments  $\{\langle \hat{A}^k \rangle_w\}_{k=1}^n$  fully characterizes the weak-valued probability distribution  $\{p_{wj}\}_{j=1}^n$ , which is similar to the relation between the set of the moments  $\{\langle \hat{A}^k \rangle\}_{k=1}^n$  and the probability distribution  $\{p_j\}_{j=1}^n$ . The *n*-th order weak moment  $\langle \hat{A}^n \rangle_w$  can be experimentally observed in the indirect measurement setup by taking into consideration the terms up to the *n*-th order of  $\theta$  in Eq. (3). The physical meaning of the weak moment may be somewhat elusive as well as the weak values; nevertheless, the weak moment could be possible to provide a new perspective on fundamental problems in quantum mechanics. For example, Scully *et al.*'s claim that the momentum disturbance associated with which-way measurement in Young's double-slit experiment can be avoided [47] has been justified by the fact that the weak-valued probabilities corresponding to the momentum disturbance have zero variance due to their negativeness [12, 13]. These

studies are implicitly based on the idea of the weak variance (second-order weak moment). In a similar way, the weak moment is expected to play an important role in other problems of this kind. In addition, the use of measurement methods other than the weak measurements with Gaussian probes—such as weak measurement using a qubit probe [48] and the method without a probe [49]—may find new implications for the weak moments.

Finally, as an application of the weak moments  $\langle \hat{A}^n \rangle_w$ , we propose the control of the probe wave packet by pre- and postselection of the target system. So far, several studies have been reported to narrow the probe wave packet by appropriately pre- and postselecting the target system in the weak measurement setup [22, 23, 50]. In Eq. (3), if the higher-order weak moments included in the  $O(\theta^2)$  term are properly controlled, any waveform of the probe can be configured (for detail, see Appendix E). For example, the non-Gaussian states in the quadrature amplitude of light, such as the cat state [51, 52] and the Gottesman–Kitaev–Preskill state [53], play an important role in quantum optics, and our method may provide a new construction method for their realization.

## ACKNOWLEDGMENTS

This research was supported by JSPS KAKENHI Grant Number 16K17524 and 19K14606, the Matsuo Foundation, and the Research Foundation for Opto-Science and Technology.

## Appendix A: Change of probe wave packet in indirect measurement for mixed pre- and postselected systems

We calculate the expectation value  $\langle \hat{M} \rangle_f$  and the variance  $\sigma_f^2(\hat{M})$  of the probe wave packet in the indirect measurement, when the pre- and postselected states are mixed states represented by the density operators  $\hat{\rho}_i$  and  $\hat{\rho}_f$ , respectively. When  $\hat{\rho}_i = |i\rangle\langle i|$  and  $\hat{\rho}_f = |f\rangle\langle f|$ , it corresponds to the case of the pure pre- and postselected states, and when  $\hat{\rho}_f = \hat{1}/d$ , the case of the preselection only. The time evolution of the whole state is calculated as:

$$\begin{aligned}
& \hat{\rho}_i \otimes |\phi\rangle\langle\phi| \\
& \xrightarrow{\text{Interaction}} \exp(-i\theta\hat{A} \otimes \hat{K}) (\hat{\rho}_i \otimes |\phi\rangle\langle\phi|) \exp(i\theta\hat{A} \otimes \hat{K}) \\
& \xrightarrow{\text{Postselection}} \text{tr}_t \left[ \hat{\rho}_f \exp(-i\theta\hat{A} \otimes \hat{K}) (\hat{\rho}_i \otimes |\phi\rangle\langle\phi|) \exp(i\theta\hat{A} \otimes \hat{K}) \right] \\
& = \text{tr}(\hat{\rho}_f \hat{\rho}_i) \left[ |\phi\rangle\langle\phi| + \left( -i\theta\langle\hat{A}\rangle_w \hat{K} |\phi\rangle\langle\phi| - \frac{1}{2}\theta^2\langle\hat{A}^2\rangle_w \hat{K}^2 |\phi\rangle\langle\phi| \right) + \text{H.c.} + \theta^2 \tilde{A} \hat{K} |\phi\rangle\langle\phi| \hat{K} \right] + O(\theta^3) \\
& =: \tilde{\rho}_\phi, \tag{A1}
\end{aligned}$$

where  $\text{tr}_t$  denotes the partial trace for the target system, and H.c. represents the Hermitian conjugate of the preceding term.  $\langle\hat{A}\rangle_w = \text{tr}(\hat{\rho}_f \hat{A} \hat{\rho}_i) / \text{tr}(\hat{\rho}_f \hat{\rho}_i)$  is the weak value of  $\hat{A}$  for the pre- and postselected system represented by the density operators  $\hat{\rho}_i$  and  $\hat{\rho}_f$ . We define  $\tilde{A} := \text{tr}(\hat{\rho}_f \hat{A} \hat{\rho}_i \hat{A}) / \text{tr}(\hat{\rho}_f \hat{\rho}_i)$ ; when  $\hat{\rho}_i$  and  $\hat{\rho}_f$  are pure,  $\tilde{A} = |\langle\hat{A}\rangle_w|^2$ , and when  $\hat{\rho}_f = \hat{1}/d$  (completely mixed state),  $\tilde{A} = \text{tr}(\hat{\rho}_i \hat{A}^2) = \langle\hat{A}^2\rangle$ .

The expectation value of  $\hat{M}$  for the unnormalized probe state  $\tilde{\rho}_\phi$  is expressed as  $\langle\hat{M}\rangle_f = \text{tr}(\tilde{\rho}_\phi \hat{M}) / \text{tr}(\tilde{\rho}_\phi)$ . The numerator  $\text{tr}(\tilde{\rho}_\phi \hat{M})$  is calculated as

$$\text{tr}(\tilde{\rho}_\phi \hat{M}) = \text{tr}(\hat{\rho}_f \hat{\rho}_i) \left[ \langle\hat{M}\rangle + \left( -i\theta\langle\hat{A}\rangle_w \langle\hat{M}\hat{K}\rangle - \frac{1}{2}\theta^2\langle\hat{A}^2\rangle_w \langle\hat{M}\hat{K}^2\rangle \right) + \text{c.c.} + \theta^2 \tilde{A} \langle\hat{K}\hat{M}\hat{K}\rangle \right] + O(\theta^3), \tag{A2}$$

where c.c. represents the complex conjugate of the preceding term. Because the expectation value of the product of odd numbers of  $\hat{X}$  or  $\hat{K}$  for our Gaussian probe state becomes zero, for  $\hat{M} = \hat{X} \cos \alpha + \hat{K} \sin \alpha$ , the above equation can be reduced as

$$\text{tr}(\tilde{\rho}_\phi \hat{M}) = \text{tr}(\hat{\rho}_f \hat{\rho}_i) \left[ \left( -i\theta\langle\hat{A}\rangle_w \langle\hat{M}\hat{K}\rangle \right) + \text{c.c.} \right] + O(\theta^3). \tag{A3}$$

A similar calculation yields the denominator  $\text{tr}(\tilde{\rho}_\phi)$  as

$$\text{tr}(\tilde{\rho}_\phi) = \text{tr}(\hat{\rho}_f \hat{\rho}_i) \left[ 1 + \left( -\frac{1}{2}\theta^2\langle\hat{A}^2\rangle_w \langle\hat{K}^2\rangle \right) + \text{c.c.} + \theta^2 \tilde{A} \langle\hat{K}^2\rangle \right] + O(\theta^3). \tag{A4}$$

Therefore, the expectation value  $\langle\hat{M}\rangle_f$  is expressed as

$$\langle\hat{M}\rangle_f = \frac{\text{tr}(\tilde{\rho}_\phi \hat{M})}{\text{tr}(\tilde{\rho}_\phi)} = \left( -i\theta\langle\hat{A}\rangle_w \langle\hat{M}\hat{K}\rangle \right) + \text{c.c.} + O(\theta^3), \tag{A5}$$

where we used the following formula:

$$\frac{a_0 + a_1\theta + a_2\theta^2 + O(\theta^3)}{b_0 + b_1\theta + b_2\theta^2 + O(\theta^3)} = \frac{a_0}{b_0} + \frac{a_1 b_0 - a_0 b_1}{b_0^2} \theta + \frac{a_2 b_0^2 - a_0 b_0 b_2 - a_1 b_0 b_1 + a_0 b_1^2}{b_0^3} \theta^2 + O(\theta^3). \tag{A6}$$

Because  $\langle\hat{M}\hat{K}\rangle = (i \cos \alpha + \sin \alpha)/2$  for our Gaussian probe state, we obtain a concrete form of  $\langle\hat{M}\rangle_f$  as follows:

$$\langle\hat{M}\rangle_f = \frac{1}{2}\theta\langle\hat{A}\rangle_w (\cos \alpha - i \sin \alpha) + \text{c.c.} + O(\theta^3) = \theta \left( \text{Re}\langle\hat{A}\rangle_w \cos \alpha + \text{Im}\langle\hat{A}\rangle_w \sin \alpha \right) + O(\theta^3), \tag{A7}$$

which matches Eq. (4) in the main text.

The variance of  $\hat{M}$  for the unnormalized probe state  $\tilde{\rho}_\phi$  is expressed as  $\sigma_f^2(\hat{M}) = \langle\hat{M}^2\rangle_f - \langle\hat{M}\rangle_f^2$ . The first term is



calculated as

$$\begin{aligned}
\langle \hat{M}^2 \rangle_f &= \frac{\text{tr}(\tilde{\rho}_\phi \hat{M}^2)}{\text{tr}(\tilde{\rho}_\phi)} \\
&= \frac{\langle \hat{M}^2 \rangle + \left( -\frac{1}{2}\theta^2 \langle \hat{A}^2 \rangle_w \langle \hat{M}^2 \hat{K}^2 \rangle \right) + \text{c.c.} + \theta^2 \tilde{A} \langle \hat{K} \hat{M}^2 \hat{K} \rangle + O(\theta^3)}{1 + \left( -\frac{1}{2}\theta^2 \langle \hat{A}^2 \rangle_w \langle \hat{K}^2 \rangle \right) + \text{c.c.} + \theta^2 \tilde{A} \langle \hat{K}^2 \rangle + O(\theta^3)} \\
&= \langle \hat{M}^2 \rangle + \left( -\frac{1}{2}\theta^2 \langle \hat{A}^2 \rangle_w \langle \hat{M}^2 \hat{K}^2 \rangle \right) + \text{c.c.} + \theta^2 \tilde{A} \langle \hat{K} \hat{M}^2 \hat{K} \rangle + \langle \hat{M}^2 \rangle \left( \frac{1}{2}\theta^2 \langle \hat{A}^2 \rangle_w \langle \hat{K}^2 \rangle + \text{c.c.} - \theta^2 \tilde{A} \langle \hat{K}^2 \rangle \right) + O(\theta^3).
\end{aligned} \tag{A8}$$

Because the following equations hold for our Gaussian probe state:

$$\langle \hat{M}^2 \rangle = \langle \hat{K}^2 \rangle = \frac{1}{2}, \quad \langle \hat{M}^2 \hat{K} \rangle = \frac{1}{4} - \frac{1}{2} [\cos(2\alpha) - i \sin(2\alpha)], \quad \text{and} \quad \langle \hat{K} \hat{M}^2 \hat{K} \rangle = \frac{3}{4}, \tag{A9}$$

we obtain the following expression:

$$\langle \hat{M}^2 \rangle_f = \frac{\text{tr}(\tilde{\rho}_\phi \hat{M}^2)}{\text{tr}(\tilde{\rho}_\phi)} = \frac{1}{2} + \frac{1}{2}\theta^2 \cos(2\alpha) \text{Re} \langle \hat{A}^2 \rangle_w + \frac{1}{2}\theta^2 \sin(2\alpha) \text{Im} \langle \hat{A}^2 \rangle_w + \frac{1}{2}\theta^2 \tilde{A} + O(\theta^3). \tag{A10}$$

The second term  $\langle \hat{M} \rangle_f^2$  is calculated by using Eq. (A7) as

$$\langle \hat{M} \rangle_f^2 = \frac{1}{2}\theta^2 \left[ \left( \text{Re} \langle \hat{A} \rangle_w \right)^2 - \left( \text{Im} \langle \hat{A} \rangle_w \right)^2 \right] \cos(2\alpha) + \theta^2 \text{Re} \langle \hat{A} \rangle_w \text{Im} \langle \hat{A} \rangle_w \sin(2\alpha) + \frac{1}{2}\theta^2 |\langle \hat{A} \rangle_w|^2 + O(\theta^3). \tag{A11}$$

Therefore, we obtain the concrete form of  $\sigma_f^2(\hat{M})$  as

$$\begin{aligned}
\sigma_f^2(\hat{M}) &= \langle \hat{M}^2 \rangle_f - \langle \hat{M} \rangle_f^2 \\
&= \frac{1}{2} + \frac{1}{2}\theta^2 \cos(2\alpha) \left[ \text{Re} \langle \hat{A}^2 \rangle_w - \left( \text{Re} \langle \hat{A} \rangle_w \right)^2 + \left( \text{Im} \langle \hat{A} \rangle_w \right)^2 \right] \\
&\quad + \frac{1}{2}\theta^2 \sin(2\alpha) \left[ \text{Im} \langle \hat{A}^2 \rangle_w - 2\text{Re} \langle \hat{A} \rangle_w \text{Im} \langle \hat{A} \rangle_w \right] + \frac{1}{2}\theta^2 \left( \tilde{A} - |\langle \hat{A} \rangle_w|^2 \right) + O(\theta^3) \\
&= \frac{1}{2} + \frac{1}{2}\theta^2 \cos(2\alpha) \text{Re} \sigma_w^2(\hat{A}) + \frac{1}{2}\theta^2 \sin(2\alpha) \text{Im} \sigma_w^2(\hat{A}) + \frac{1}{2}\theta^2 \left( \tilde{A} - |\langle \hat{A} \rangle_w|^2 \right) + O(\theta^3),
\end{aligned} \tag{A12}$$

where we used the following formulae:

$$\text{Re} \sigma_w^2(\hat{A}) = \text{Re} \langle \hat{A}^2 \rangle_w - \left( \text{Re} \langle \hat{A} \rangle_w \right)^2 + \left( \text{Im} \langle \hat{A} \rangle_w \right)^2, \tag{A13}$$

$$\text{Im} \sigma_w^2(\hat{A}) = \text{Im} \langle \hat{A}^2 \rangle_w - 2\text{Re} \langle \hat{A} \rangle_w \text{Im} \langle \hat{A} \rangle_w. \tag{A14}$$

In particular, when  $\hat{\rho}_i$  and  $\hat{\rho}_f$  are pure,  $\tilde{A} = |\langle \hat{A} \rangle_w|^2$  and thus Eq. (A12) matches Eq. (7) in the main text. On the other hand, when  $\hat{\rho}_f = \hat{1}/d$  (case of preselection only),  $\tilde{A} = \langle \hat{A}^2 \rangle$ ,  $\langle \hat{A} \rangle_w = \langle \hat{A} \rangle$ , and  $\sigma_w^2(\hat{A}) = \sigma^2(\hat{A}) \in \mathbb{R}$ ; therefore,

$$\sigma_f^2(\hat{M}) = \frac{1}{2} + \frac{1}{2}\theta^2 \cos(2\alpha) \sigma^2(\hat{A}) + \frac{1}{2}\theta^2 \sigma^2(\hat{A}) + O(\theta^3). \tag{A15}$$

When  $\alpha = 0$ , we obtain

$$\sigma_f^2(\hat{M}) = \sigma_f^2(\hat{X}) = \frac{1}{2} + \theta^2 \sigma^2(\hat{A}) + O(\theta^3), \tag{A16}$$

which is equal to  $\sigma_f^2(\hat{X})$  in Eq. (2) in the main text except for the  $O(\theta^3)$  term (this term vanishes in the full-order expansion in this case). We note that if the probe state is not the Gaussian wave packet, the expectation value and variance of  $\hat{M}$  for the probe wave packet after the postselection will not be Eqs. (A7) and (A12), respectively.

## Appendix B: Fractional Fourier transform and its optical realization

### 1. Definition of fractional Fourier transform

For any real number  $\alpha$ , the  $\alpha$ -angle fractional Fourier transform of a function  $\phi$  is defined by

$$\mathcal{F}_\alpha[\phi](\omega) := \sqrt{\frac{1 - i \cot(\alpha)}{2\pi}} \int_{-\infty}^{\infty} dx \phi(x) \exp \left[ i \left( \frac{\cot(\alpha)\omega^2 - 2 \csc(\alpha)\omega x + \cot(\alpha)x^2}{2} \right) \right], \quad (\text{B1})$$

where  $x$  and  $\omega$  are dimensionless variables,  $\cot(\alpha) = 1/\tan(\alpha)$ , and  $\csc(\alpha) = 1/\sin(\alpha)$ . We also define  $\phi_\alpha$  as the function into which the function  $\phi_0$  is transformed by  $\mathcal{F}_\alpha$ . In particular, when  $\alpha = \pi/2$ ,  $\mathcal{F}_\alpha$  is reduced to the normal Fourier transform  $\mathcal{F}$ :

$$\mathcal{F}_{\pi/2}[\phi_0](\omega) = \phi_{\pi/2}(\omega) = \frac{1}{\sqrt{2\pi}} \int_{-\infty}^{\infty} dx \phi_0(x) e^{-i\omega x} = \mathcal{F}[\phi_0](\omega). \quad (\text{B2})$$

When  $\alpha = \pm\pi/4$  and  $\alpha = \pm 3\pi/4$ , the fractional Fourier transform is respectively expressed as

$$\mathcal{F}_{\pm\pi/4}[\phi_0](\omega) = \phi_{\pm\pi/4}(\omega) = \sqrt{\frac{1 \mp i}{2\pi}} \int_{-\infty}^{\infty} dx \phi_0(x) \exp \left[ \pm i \left( \frac{\omega^2 - 2\sqrt{2}\omega x + x^2}{2} \right) \right], \quad (\text{B3})$$

$$\mathcal{F}_{\pm 3\pi/4}[\phi_0](\omega) = \phi_{\pm 3\pi/4}(\omega) = \sqrt{\frac{1 \pm i}{2\pi}} \int_{-\infty}^{\infty} dx \phi_0(x) \exp \left[ \mp i \left( \frac{\omega^2 + 2\sqrt{2}\omega x + x^2}{2} \right) \right]. \quad (\text{B4})$$

We call  $\mathcal{F}_{\pm\pi/4}$  and  $\mathcal{F}_{\pm 3\pi/4}$  as  $\pm 1/2$ - and  $\pm 3/2$ -Fourier transform, respectively.

### 2. Relationship between observables $\hat{X}$ , $\hat{K}$ , $\hat{\Omega}$ , and $\hat{\Xi}$

For an observable  $\hat{X}$ , its canonical conjugate observable  $\hat{K}$  is defined as the observable that satisfies the canonical commutation relation  $[\hat{X}, \hat{K}] = i\hat{1}$ .  $\hat{X}$  and  $\hat{K}$  are spectrally decomposed as follows:

$$\hat{X} = \int_{-\infty}^{\infty} dX X |X\rangle \langle X|, \quad \hat{K} = \int_{-\infty}^{\infty} dK K |K\rangle \langle K|. \quad (\text{B5})$$

Their eigenvectors  $|X\rangle$  and  $|K\rangle$  are related to each other by the Fourier transform:

$$|K\rangle = \mathcal{F}_{-\pi/2}[|X\rangle](K) = \frac{1}{\sqrt{2\pi}} \int_{-\infty}^{\infty} dX |X\rangle e^{iKX}. \quad (\text{B6})$$

$\hat{\Omega}$  and  $\hat{\Xi}$  are defined as

$$\hat{\Omega} := \frac{\hat{X} + \hat{K}}{\sqrt{2}}, \quad \hat{\Xi} := \frac{-\hat{X} + \hat{K}}{\sqrt{2}}. \quad (\text{B7})$$

They satisfy the canonical commutation relation  $[\hat{\Omega}, \hat{\Xi}] = i\hat{1}$ .  $\hat{\Omega}$  and  $\hat{\Xi}$  spectrally decomposed as follows:

$$\hat{\Omega} = \int_{-\infty}^{\infty} d\Omega \Omega |\Omega\rangle \langle \Omega|, \quad \hat{\Xi} = \int_{-\infty}^{\infty} d\Xi \Xi |\Xi\rangle \langle \Xi|. \quad (\text{B8})$$

Their eigenvector  $|\Omega\rangle$  and  $|\Xi\rangle$  are related to  $|X\rangle$  by the  $-1/2$ - and  $-3/2$ -Fourier transform, respectively:

$$|\Omega\rangle = \mathcal{F}_{-\pi/4}[|X\rangle](\Omega) = \sqrt{\frac{1+i}{2\pi}} \int_{-\infty}^{\infty} dX |X\rangle \exp \left[ -i \left( \frac{\Omega^2 - 2\sqrt{2}\Omega X + X^2}{2} \right) \right], \quad (\text{B9})$$

$$|\Xi\rangle = \mathcal{F}_{-3\pi/4}[|X\rangle](\Xi) = \sqrt{\frac{1-i}{2\pi}} \int_{-\infty}^{\infty} dX |X\rangle \exp \left[ i \left( \frac{\Xi^2 + 2\sqrt{2}\Xi X + X^2}{2} \right) \right]. \quad (\text{B10})$$

When the state  $|\phi\rangle$  is expanded in each basis as  $|\phi\rangle = \int_{-\infty}^{\infty} dX \phi_0(X)|X\rangle = \int_{-\infty}^{\infty} d\Omega \phi_{\pi/4}(\Omega)|\Omega\rangle = \int_{-\infty}^{\infty} dK \phi_{\pi/2}(K)|K\rangle = \int_{-\infty}^{\infty} d\Xi \phi_{3\pi/4}(\Xi)|\Xi\rangle$ , the relation between each wavefunction and basis vector is summarized as follows:

$$\phi_0(X) \xrightarrow{\mathcal{F}_{\pi/4}} \phi_{\pi/4}(\Omega) \xrightarrow{\mathcal{F}_{\pi/4}} \phi_{\pi/2}(K) \xrightarrow{\mathcal{F}_{\pi/4}} \phi_{3\pi/4}(\Xi), \quad (\text{B11})$$

$$|X\rangle \xrightarrow{\mathcal{F}_{-\pi/4}} |\Omega\rangle \xrightarrow{\mathcal{F}_{-\pi/4}} |K\rangle \xrightarrow{\mathcal{F}_{-\pi/4}} |\Xi\rangle. \quad (\text{B12})$$

### 3. Optical realization of measurement of observables $\hat{X}$ , $\hat{K}$ , $\hat{\Omega}$ , and $\hat{\Xi}$

We describe how to optically realize the measurement of observables  $\hat{X}$ ,  $\hat{K}$ ,  $\hat{\Omega}$ , and  $\hat{\Xi}$  for the photon beam with transverse distribution state  $|\phi\rangle$ . The measurement of  $\hat{X}$ , which is the dimensionless transverse position observable, can be realized by measuring the photon's transverse position using a photon detector with spatial resolution. The measurement of  $\hat{K}$  can be realized by optically Fourier-transforming the photon's wavefunction  $\phi_0(X) = \langle X|\phi\rangle$  into  $\phi_{\pi/2}(K)$  and measuring its transverse position. The optical Fourier transform is realized by the combination of lens passage and free-space propagation. In a similar manner, the measurement of  $\hat{\Omega}$  and  $\hat{\Xi}$  can be realized by optically  $1/2$ - and  $3/2$ -Fourier-transforming  $\phi_0(X)$  into  $\phi_{\pi/4}(\Omega)$  and  $\phi_{3\pi/4}(\Xi)$ , respectively, and measuring its transverse position. In the following, we describe how to realize the optical  $1/2$ - and  $3/2$ -Fourier transform by the combination of lens passage and free-space propagation.

We assume that the beam is propagating in the  $z$  direction.  $x$ ,  $k$ , and  $k_x$  are the transverse position, the total wavenumber, and the  $x$  component of the wavevector, respectively. We apply the paraxial approximation and assume that  $k$  does not depend on  $k_x$  because  $k_x \ll k$ . We define the dimensionless variables  $X := xk$  and  $K_x := k_x/k$ . The free-space propagation by the distance  $d$  is represented in the wavenumber space by the following transfer function:

$$H_D^{\text{free}}(K_x) \propto \exp \left( -i \frac{DK_x^2}{2} \right), \quad (\text{B13})$$

where  $D := dk$  is a dimensionless distance. In the position space, this free-space propagation is also represented by the convolution with the following function:

$$h_D^{\text{free}}(X) \propto \int_{-\infty}^{\infty} dK_x H_D^{\text{free}}(K_x) e^{iK_x X} \propto \exp \left( i \frac{X^2}{2D} \right). \quad (\text{B14})$$

On the other hand, passing through a lens with focal length  $f$  is represented in the position space by the following transfer function:

$$h_F^{\text{lens}}(X) \propto \exp \left( -i \frac{X^2}{2F} \right), \quad (\text{B15})$$

where  $F := fk$  is a dimensionless focal length. In the wavevector space, passing through this lens is also represented by the convolution with the following function:

$$H_F^{\text{lens}}(K_x) \propto \int_{-\infty}^{\infty} dX h_F^{\text{lens}}(X) e^{-iK_x X} \propto \exp \left( i \frac{FK_x^2}{2} \right). \quad (\text{B16})$$

If a photon with a transverse wavefunction  $\phi_0(X)$  passes through a lens with focal length  $f$ , propagates in free space by

distance  $d$ , and passes through another lens with focal length  $f$  in that order, the resultant wavefunction is calculated as follows:

$$\phi_0(X) \xrightarrow{\text{lens } f} \phi_0(X) \exp\left(-i\frac{X^2}{2F}\right) \quad (\text{B17})$$

$$\xrightarrow{\text{free-space propagation } d} \int_{-\infty}^{\infty} dX' \phi_0(X') \exp\left(-i\frac{X'^2}{2F}\right) \exp\left[i\frac{(X-X')^2}{2D}\right] \quad (\text{B18})$$

$$\begin{aligned} &\xrightarrow{\text{lens } f} \int_{-\infty}^{\infty} dX' \phi_0(X') \exp\left(-i\frac{X'^2}{2F}\right) \exp\left[i\frac{(X-X')^2}{2D}\right] \exp\left(-i\frac{X^2}{2F}\right) \\ &= \int_{-\infty}^{\infty} dX' \phi_0(X') \exp\left[i\frac{(F-D)X^2 - 2FXX' + (F-D)X'^2}{2FD}\right]. \end{aligned} \quad (\text{B19})$$

If we choose  $D = F$ , we can realize the normal Fourier transform of  $\phi_0$  as follows:

$$\text{Eq. (B19)} = \int_{-\infty}^{\infty} dX' \phi_0(X') \exp\left(i\frac{-XX'}{F}\right) \propto \mathcal{F}_{\pi/2}[\phi_0]\left(\frac{X}{F}\right) = \phi_{\pi/2}\left(\frac{X}{F}\right). \quad (\text{B20})$$

The scale of the wavefunction after the Fourier transform can be adjusted by the focal length  $F$ . If we choose  $D = (1 - 1/\sqrt{2})F$ ,

$$\begin{aligned} \text{Eq. (B19)} &= \int_{-\infty}^{\infty} dX' \phi_0(X') \exp\left[i\frac{X^2 - 2\sqrt{2}XX' + X'^2}{(2 - \sqrt{2})F}\right] \\ &= \int_{-\infty}^{\infty} dX' \phi_0(X') \exp\left\{\frac{i}{2}\left[\left(\frac{X}{\sqrt{(\sqrt{2}-1)F}}\right)^2 - 2\sqrt{2}\left(\frac{X}{\sqrt{(\sqrt{2}-1)F}}\right)\left(\frac{X'}{\sqrt{(\sqrt{2}-1)F}}\right) + \left(\frac{X'}{\sqrt{(\sqrt{2}-1)F}}\right)^2\right]\right\} \\ &\propto \mathcal{F}_{\pi/4}[\phi_{0,F}^-]\left(\frac{X}{\sqrt{(\sqrt{2}-1)F}}\right) \left[\phi_{0,F}^-(X) := \phi_0\left(X\sqrt{(\sqrt{2}-1)F}\right)\right] \\ &= \phi_{\pi/4,F}^-\left(\frac{X}{\sqrt{(\sqrt{2}-1)F}}\right), \end{aligned} \quad (\text{B21})$$

where  $\phi_{0,F}^-(X)$  is a scaled wavefunction of  $\phi_0(X)$ . In this manner, we can realize the 1/2-Fourier transform of  $\phi_{F,0}(X)$ . Similarly, if we choose  $D = (1 + 1/\sqrt{2})F$ , we can realize the 3/2-Fourier transform as follows:

$$\begin{aligned} \text{Eq. (B19)} &= \int_{-\infty}^{\infty} dX' \phi_0(X') \exp\left[-i\frac{X^2 + 2\sqrt{2}XX' + X'^2}{(2 + \sqrt{2})F}\right] \\ &= \int_{-\infty}^{\infty} dX' \phi_0(X') \exp\left\{-\frac{i}{2}\left[\left(\frac{X}{\sqrt{(\sqrt{2}+1)F}}\right)^2 + 2\sqrt{2}\left(\frac{X}{\sqrt{(\sqrt{2}+1)F}}\right)\left(\frac{X'}{\sqrt{(\sqrt{2}+1)F}}\right) + \left(\frac{X'}{\sqrt{(\sqrt{2}+1)F}}\right)^2\right]\right\} \\ &\propto \mathcal{F}_{3\pi/4}[\phi_{0,F}^+]\left(\frac{X}{\sqrt{(\sqrt{2}+1)F}}\right) \left[\phi_{0,F}^+(X) := \phi_0\left(X\sqrt{(\sqrt{2}+1)F}\right)\right] \\ &= \phi_{3\pi/4,F}^-\left(\frac{X}{\sqrt{(\sqrt{2}+1)F}}\right), \end{aligned} \quad (\text{B22})$$

where  $\phi_{0,F}^+(X)$  is a scaled wavefunction of  $\phi_0(X)$ .

It should be noted that the second lens, which causes phase modulation in the position space, does not affect the result of intensity (projection) measurement in the position basis. Therefore, in our experiment in the main text, the

intensity measurements of the beam's transverse distribution in  $\hat{X}$ ,  $\hat{\Omega}$ ,  $\hat{K}$  and  $\hat{\Xi}$  bases have been realized by using only one lens followed by free-space propagation.

### Appendix C: Derivation of theoretical values of expectation value and variance of probe system in our experiment

First, we derive the exact formula of the weak value and the weak variance in our experimental setup. According to our experiment, we assume the pre- and postselected states  $\{|i\rangle, |f\rangle\}$  and the observable  $\hat{A}$  as

$$|i\rangle = \cos \frac{\vartheta_i}{2} |0\rangle + e^{i\varphi_i} \sin \frac{\vartheta_i}{2} |1\rangle, \quad |f\rangle = \frac{1}{\sqrt{2}}(|0\rangle + |1\rangle), \quad \hat{A} = |0\rangle\langle 0| - |1\rangle\langle 1|. \quad (\text{C1})$$

The weak value and the weak variance are calculated as

$$\langle \hat{A} \rangle_w = \frac{\cos \vartheta_i + i \sin \vartheta_i \sin \varphi_i}{1 + \sin \vartheta_i \cos \varphi_i}, \quad (\text{C2})$$

$$\sigma_w^2(\hat{A}) = \frac{2 \sin \vartheta_i (\sin \vartheta_i + \cos \varphi_i) - i \sin(2\vartheta_i) \sin \varphi_i}{(1 + \sin \vartheta_i \cos \varphi_i)^2}. \quad (\text{C3})$$

In our experiment, we used the following values:

$$\vartheta_i = \begin{cases} 4\vartheta_H - \pi/2 & [\text{case (i)}] \\ 2\vartheta_Q - \pi/2 & [\text{case (ii)}] \end{cases}, \quad \varphi_i = \begin{cases} 0 & [\text{case (i)}] \\ -2\vartheta_Q & [\text{case (ii)}] \end{cases}. \quad (\text{C4})$$

By substituting them for Eqs. (C2) and (C3), we obtain Eqs. (8) and (9).

Next, we derive the theoretical values of the expectation value and the variance of the probe wave packet in our experiment. The state of the whole system after the interaction is

$$\exp(-i\theta \hat{A} \otimes \hat{K}) |i\rangle |\phi\rangle = \cos \frac{\vartheta_i}{2} |0\rangle \exp(-i\theta \hat{K}) |\phi\rangle + e^{i\varphi_i} \sin \frac{\vartheta_i}{2} |1\rangle \exp(i\theta \hat{K}) |\phi\rangle. \quad (\text{C5})$$

Suppose that the first and second terms on the right-hand side of Eq. (C5) are denoted by  $|\Phi_0\rangle$  and  $|\Phi_1\rangle$ , respectively. Considering the decrease in visibility  $V \in [0, 1]$ , the state of the whole system after the interaction is expressed by the density operator as

$$\hat{\rho} := |\Phi_0\rangle\langle \Phi_0| + |\Phi_1\rangle\langle \Phi_1| + V (|\Phi_0\rangle\langle \Phi_1| + |\Phi_1\rangle\langle \Phi_0|). \quad (\text{C6})$$

After the target system is postselected onto  $|f\rangle$ , the unnormalized probe state is given as  $\tilde{\rho}_f := |f\rangle\langle \rho|f\rangle$ . We assume that the initial probe state is Gaussian distribution  $\langle X|\phi\rangle = \phi(X) = \pi^{-1/4} \exp(-X^2/2)$ . The expectation value of the observable  $\hat{M} = \hat{X} \cos \alpha + \hat{K} \sin \alpha$  for  $\tilde{\rho}_f$  is calculated as

$$\langle \hat{M} \rangle_f = \frac{\text{tr}(\tilde{\rho}_f \hat{M})}{\text{tr}(\tilde{\rho}_f)} = \theta \frac{\cos \alpha \cos \vartheta_i + V \sin \alpha \sin \vartheta_i \sin \varphi_i e^{-\theta^2}}{1 + V \sin \vartheta_i \cos \varphi_i e^{-\theta^2}}. \quad (\text{C7})$$

The theoretical values of the expectation value in the case (i) is obtained by substituting Eq. (C4) as

$$\langle \hat{M} \rangle_f = \theta \frac{\cos \alpha \sin(4\vartheta_H)}{1 - V \cos(4\vartheta_H) e^{-\theta^2}}. \quad (\text{C8})$$

We fitted this function to the measured data with  $V$  and  $\theta$  as the fitting parameters, and then obtained  $V = 0.999$

and  $\theta = 0.032$ . On the other hand, The variance of the observable  $\hat{M}$  for  $\tilde{\rho}_f$  is calculated as

$$\begin{aligned}\sigma_f^2(\hat{M}) &= \langle \hat{M}^2 \rangle_f - \langle \hat{M} \rangle_f^2 \\ &= \frac{1}{2} + \theta^2 \frac{\sin \vartheta_i \left\{ \left( \cos^2 \alpha - V^2 \sin^2 \alpha e^{-2\theta^2} \right) \sin \vartheta_i + V e^{-\theta^2} [\cos(2\alpha) \cos \varphi_i + \sin(2\alpha) \cos \vartheta_i \sin \varphi_i] \right\}}{(1 + V \sin \vartheta_i \cos \varphi_i e^{-\theta^2})^2}.\end{aligned}\quad (\text{C9})$$

Substituting Eq. (C4), the theoretical values of the variance in the case (i) is obtained as

$$\sigma_f^2(\hat{M}) = \frac{1}{2} + \theta^2 \frac{\cos(4\vartheta_H) \left[ \left( \cos^2 \alpha - V^2 e^{-2\theta^2} \sin^2 \alpha \right) \cos(4\vartheta_H) - V e^{-\theta^2} \cos(2\alpha) \right]}{[1 - V \cos(4\vartheta_H) e^{-\theta^2}]^2}, \quad (\text{C10})$$

and that in case (ii) as

$$\sigma_f^2(\hat{M}) = \frac{1}{2} + \theta^2 \frac{\cos(2\vartheta_Q) \left\{ \left( \cos^2 \alpha - V^2 e^{-2\theta^2} \sin^2 \alpha \right) \cos(2\vartheta_Q) - V e^{-\theta^2} [\cos(2\alpha) \cos(2\vartheta_Q) - \sin(2\alpha) \sin^2(2\vartheta_Q)] \right\}}{[1 - V \cos^2(2\vartheta_Q) e^{-\theta^2}]^2}.\quad (\text{C11})$$

We fitted these functions to the measured data with  $V$  as the fitting parameter and  $\theta = 0.032$  as the fixed parameter.

#### Appendix D: Weak variance as conditional pseudo-variance of Kirkwood–Dirac distribution

We show that weak values and weak variances can be understood as conditional pseudo-expectation values and conditional pseudo-variances of Kirkwood–Dirac (KD) distribution [45, 46], respectively. The  $(j, k)$  component of the KD distribution of the state  $|i\rangle$  expanded in two orthonormal bases  $\{|a_j\rangle\}_j$  and  $\{|a'_k\rangle\}_k$  is defined as

$$D(a_j, a'_k | i) := \text{tr}(|a_j\rangle\langle a_j | a'_k\rangle\langle a'_k | i\rangle\langle i|). \quad (\text{D1})$$

The KD distribution is a joint pseudo-probability distribution that represents the quantum state  $|i\rangle$  and is generally a complex number. The sum of the KD distribution for the two indices  $j, k$  becomes unity:  $\sum_{j,k} D(a_j, a'_k | i) = 1$ . The marginal distribution of KD distribution summed for one index becomes the projection probability distribution of  $|i\rangle$  in the other basis:

$$\sum_j D(a_j, a'_k | i) = |\langle a'_k | i \rangle|^2, \quad \sum_k D(a_j, a'_k | i) = |\langle a_j | i \rangle|^2. \quad (\text{D2})$$

When we choose  $|a_j\rangle = |f\rangle$ , the conditional pseudo-probability  $D(a'_k | i, f)$  of the KD distribution is expressed as:

$$D(a'_k | i, f) := \frac{D(f, a'_k | i)}{\sum_k D(f, a'_k | i)} = \frac{\langle f | a'_k \rangle \langle a'_k | i \rangle}{\langle f | i \rangle} = p'_{wk}, \quad (\text{D3})$$

where  $\{p'_{wk}\}_k$  is the weak-valued probability distribution of the pre- and postselection system  $\{|i\rangle, |f\rangle\}$  in the orthonormal basis  $\{|a'_k\rangle\}_k$ . Therefore, the weak value  $\langle \hat{A}' \rangle_w$  and weak variance  $\sigma_w^2(\hat{A}')$  for the observable  $\hat{A}' := \sum_k a'_k |a'_k\rangle\langle a'_k|$  are represented as the conditional pseudo-expectation values and conditional pseudo-variance of the KD distribution, respectively, as follows:

$$\sum_k a'_k D(a'_k | i, f) = \sum_k a'_k p'_{wk} = \langle \hat{A}' \rangle_w, \quad (\text{D4})$$

$$\sum_k (a'_k - \langle \hat{A}' \rangle_w)^2 D(a'_k | i, f) = \sum_k (a'_k - \langle \hat{A}' \rangle_w)^2 p'_{wk} = \sigma_w^2(\hat{A}'). \quad (\text{D5})$$

### Appendix E: Control of probe wavefunction by pre- and postselection of target system

We explain that, in indirect measurement for pre- and postselected systems, the probe state after the postselection can be controlled by appropriately choosing the pre- and postselection. The wavefunction in the  $\hat{K}$  basis of the probe state after the postselection  $|\tilde{\phi}\rangle$  [Eq. (3) in the main text],  $\tilde{\phi}(K)$ , is expressed for all orders of  $\theta$  as

$$\tilde{\phi}(K) = \langle K|\tilde{\phi}\rangle = \langle K|\left[\langle f|i\rangle\sum_{n=0}^{\infty}\frac{(-i\theta)^n}{n!}\langle\hat{A}^n\rangle_w\hat{K}^n|\phi\rangle\right] = \langle f|i\rangle\sum_{n=0}^{\infty}\frac{(-i\theta)^n}{n!}\langle\hat{A}^n\rangle_w K^n\phi(K). \quad (\text{E1})$$

Let  $\phi_*(K)$  be the wavefunction in the  $\hat{K}$  basis of the desired probe state. To realize  $\phi_*(K)$  except for a constant multiple, we can choose the weak moments  $\{\langle\hat{A}^n\rangle_w\}_n$  so that

$$\sum_{n=0}^{\infty}\frac{(-i\theta)^n}{n!}\langle\hat{A}^n\rangle_w K^n \propto \frac{\phi_*(K)}{\phi(K)}. \quad (\text{E2})$$

When the target system is  $d$ -dimensional, if  $\hat{A}$  has full rank, we can choose the values of  $d$  weak moments  $\langle\hat{A}^n\rangle_w$  independently. Therefore, by fixing the values of the weak moments of the low-order term of  $\theta$  ( $n = 1, \dots, d$ ) appropriately, which has a large effect on the waveform, the desired wavefunction can be approximately realized.

- 
- [1] J. A. Wheeler and W. H. Zurek, *Quantum theory and measurement* (Princeton University Press, 2014).
- [2] J. von Neumann, *Mathematical foundations of quantum mechanics: New edition* (Princeton university press, 2018).
- [3] Y. Aharonov, D. Z. Albert, and L. Vaidman, “How the result of a measurement of a component of the spin of a spin-1/2 particle can turn out to be 100,” *Phys. Rev. Lett.* **60**, 1351 (1988).
- [4] Y. Aharonov and L. Vaidman, “Complete description of a quantum system at a given time,” *J. Phys. A* **24**, 2315 (1991).
- [5] K. J. Resch, J. S. Lundeen, and A. M. Steinberg, “Experimental realization of the quantum box problem,” *Phys. Lett. A* **324**, 125 (2004).
- [6] J. S. Lundeen and A. M. Steinberg, “Experimental joint weak measurement on a photon pair as a probe of hardy’s paradox,” *Phys. Rev. Lett.* **102**, 020404 (2009).
- [7] K. Yokota, T. Yamamoto, M. Koashi, and N. Imoto, “Direct observation of hardy’s paradox by joint weak measurement with an entangled photon pair,” *New J. Phys.* **11**, 033011 (2009).
- [8] T. Denkmayr, H. Geppert, S. Sponar, H. Lemmel, A. Matzkin, J. Tollaksen, and Y. Hasegawa, “Observation of a quantum cheshire cat in a matter-wave interferometer experiment,” *Nat. Commun.* **5**, 5492 (2014).
- [9] R. Okamoto and S. Takeuchi, “Experimental demonstration of a quantum shutter closing two slits simultaneously,” *Sci. Rep.* **6**, 35161 (2016).
- [10] A. Danan, D. Farfurnik, S. Bar-Ad, and L. Vaidman, “Asking photons where they have been,” *Phys. Rev. Lett.* **111**, 240402 (2013).
- [11] B. L. Higgins, M. S. Palsson, G. Y. Xiang, H. M. Wiseman, and G. J. Pryde, “Using weak values to experimentally determine “negative probabilities” in a two-photon state with bell correlations,” *Phys. Rev. A* **91**, 012113 (2015).
- [12] H. M. Wiseman, “Directly observing momentum transfer in twin-slit “which-way” experiments,” *Phys. Lett. A* **311**, 285–291 (2003).
- [13] R. Mir, J. S. Lundeen, M. W. Mitchell, A. M. Steinberg, J. L. Garretson, and H. M. Wiseman, “A double-slit ‘which-way’ experiment on the complementarity–uncertainty debate,” *New J. Phys.* **9**, 287 (2007).
- [14] Y. Xiao, H. M. Wiseman, J.-S. Xu, Y. Kedem, C.-F. Li, and G.-C. Guo, “Observing momentum disturbance in double-slit “which-way” measurements,” *Sci. Adv.* **5**, eaav9547 (2019).
- [15] M. Ringbauer, D. N. Biggerstaff, M. A. Broome, A. Fedrizzi, C. Branciard, and A. G. White, “Experimental joint quantum measurements with minimum uncertainty,” *Phys. Rev. Lett.* **112**, 020401 (2014).
- [16] F. Kaneda, S.-Y. Baek, M. Ozawa, and K. Edamatsu, “Experimental test of error-disturbance uncertainty relations by weak measurement,” *Phys. Rev. Lett.* **112**, 020402 (2014).
- [17] L. A. Rozema, A. Darabi, D. H. Mahler, A. Hayat, Y. Soudagar, and A. M. Steinberg, “Violation of heisenberg’s measurement-disturbance relationship by weak measurements,” *Phys. Rev. Lett.* **109**, 100404 (2012).
- [18] S. Kocsis, B. Braverman, S. Ravets, M. J. Stevens, R. P. Mirin, L. K. Shalm, and A. M. Steinberg, “Observing the average trajectories of single photons in a two-slit interferometer,” *Science* **332**, 1170 (2011).
- [19] D. H. Mahler, L. Rozema, K. Fisher, L. Vermeyden, K. J. Resch, H. M. Wiseman, and A. M. Steinberg, “Experimental nonlocal and surreal bohmian trajectories,” *Sci. Adv.* **2**, e1501466 (2016).
- [20] J. Dressel, C. J. Broadbent, J. C. Howell, and A. N. Jordan, “Experimental violation of two-party

- leggett-garg inequalities with semiweak measurements,” *Phys. Rev. Lett.* **106**, 040402 (2011).
- [21] M. E. Goggin, M. P. Almeida, M. Barbieri, B. P. Lanyon, J. L. O’Brien, A. G. White, and G. J. Pryde, “Violation of the leggett–garg inequality with weak measurements of photons,” *PNAS* **108**, 1256 (2011).
- [22] B. de Lima Bernardo, W. S. Martins, S. Azevedo, and A. Rosas, “Uncertainty control and precision enhancement of weak measurements in the quadratic regime,” *Phys. Rev. A* **92**, 012109 (2015).
- [23] F. Matsuoka, A. Tomita, and Y. Shikano, “Generation of phase-squeezed optical pulses with large coherent amplitudes by post-selection of single photon and weak cross-kerr non-linearity,” *Quantum Stud.: Math. Found.* **4**, 159–169 (2017).
- [24] D. R. M. Arvidsson-Shukur, N. Y. Halpern, H. V. Lepage, A. A. Lasek, C. H. W. Barnes, and S. Lloyd, “Quantum negativity provides advantage in postselected metrology,” arXiv preprint arXiv:1903.02563.
- [25] N. Yunger Halpern, B. Swingle, and J. Dressel, “Quasiprobability behind the out-of-time-ordered correlator,” *Phys. Rev. A* **97**, 042105 (2018).
- [26] J. R. González Alonso, N. Yunger Halpern, and J. Dressel, “Out-of-time-ordered-correlator quasiprobabilities robustly witness scrambling,” *Phys. Rev. Lett.* **122**, 040404 (2019).
- [27] B. Reznik and Y. Aharonov, “Time-symmetric formulation of quantum mechanics,” *Phys. Rev. A* **52**, 2538–2550 (1995).
- [28] B. Reznik, “Interaction with a pre and post selected environment and recoherence,” arXiv preprint quant-ph/9501023 (1995).
- [29] A. Tanaka, “Semiclassical theory of weak values,” *Phys. Lett. A* **297**, 307–312 (2002).
- [30] A. Brodutch, “Weak measurements of non local variables,” arXiv preprint arXiv:0811.1706 (2008).
- [31] A. D. Parks, “Weak energy: form and function,” in *Quantum Theory: A Two-Time Success Story* (Springer, 2014) pp. 291–302.
- [32] Y. Aharonov and L. Vaidman, “Properties of a quantum system during the time interval between two measurements,” *Phys. Rev. A* **41**, 11–20 (1990).
- [33] A. D. Parks, “Weak covariance and the correlation of an observable with pre-selected and post-selected state energies during its time-dependent weak value measurement,” *Quantum Stud.: Math. Found.* **5**, 455–461 (2018).
- [34] M. R. Feyereisen, “How the weak variance of momentum can turn out to be negative,” *Found. Phys.* **45**, 535–556 (2015).
- [35] H. F. Hofmann, “Characterization of decoherence in a quantum channel using weak measurements,” in *International Quantum Electronics Conference* (Optical Society of America, 2011) p. I260.
- [36] H. F. Hofmann, “On the role of complex phases in the quantum statistics of weak measurements,” *New J. Phys.* **13**, 103009 (2011).
- [37] A. K. Pati and J. Wu, “Uncertainty and complementarity relations in weak measurement,” arXiv preprint arXiv:1411.7218 (2014).
- [38] Q.-C. Song and C.-F. Qiao, “Uncertainty equalities and uncertainty relation in weak measurement,” arXiv preprint arXiv:1505.02233 (2015).
- [39] P. P. Hofer, “Quasi-probability distributions for observables in dynamic systems,” *Quantum* **1**, 32 (2017).
- [40] The dimensionless variable  $X$  is obtained by dividing the position variable  $x$  by the standard deviation  $\sigma$  of the wave function  $\pi^{-1/4}\sigma^{-1/2}\exp[-x^2/(2\sigma^2)]$ .
- [41] R. Jozsa, “Complex weak values in quantum measurement,” *Phys. Rev. A* **76**, 044103 (2007).
- [42] See Appendix A for the detail when the pre- and post-selected states of the target system are mixed states.
- [43] E. H. Kennard, “Zur quantenmechanik einfacher bewegungstypen,” *Z. Phys.* **44**, 326–352 (1927).
- [44] H. P. Robertson, “The uncertainty principle,” *Phys. Rev.* **34**, 163–164 (1929).
- [45] J. G. Kirkwood, “Quantum statistics of almost classical assemblies,” *Phys. Rev.* **44**, 31–37 (1933).
- [46] P. A. M. Dirac, “On the analogy between classical and quantum mechanics,” *Rev. Mod. Phys.* **17**, 195–199 (1945).
- [47] M. O. Scully, B.-G. Englert, and H. Walther, “Quantum optical tests of complementarity,” *Nature* **351**, 111–116 (1991).
- [48] S.-J. Wu and K. Mølmer, “Weak measurements with a qubit meter,” *Phys. Lett. A* **374**, 34–39 (2009).
- [49] K. Ogawa, H. Kobayashi, and A. Tomita, “Operational formulation of weak values without probe systems,” *Phys. Rev. A* **101**, 042117 (2020).
- [50] A. D. Parks and J. E. Gray, “Variance control in weak-value measurement pointers,” *Phys. Rev. A* **84**, 012116 (2011).
- [51] B. Yurke and D. Stoler, “Generating quantum mechanical superpositions of macroscopically distinguishable states via amplitude dispersion,” *Phys. Rev. Lett.* **57**, 13–16 (1986).
- [52] W. Schleich, M. Pernigo, and F. L. Kien, “Nonclassical state from two pseudoclassical states,” *Phys. Rev. A* **44**, 2172–2187 (1991).
- [53] D. Gottesman, A. Kitaev, and J. Preskill, “Encoding a qubit in an oscillator,” *Phys. Rev. A* **64**, 012310 (2001).